

# On the Capacity of the Copper Cable Channel Using the Common Mode

T. Magesacher, P. Ödler, P. O. Börjesson, W. Henkel, T. Nordström, R. Zukunft, and S. Haar

Telecommunications Research Center Vienna (ftw.)  
 Donau-City Straße 1/III  
 A-1220 Vienna, Austria  
 magesacher@ieee.org

**Abstract**—The common-mode (CM) signal in wireline transmission systems has proven to provide valuable information exploited for mitigating narrowband noise at the receive side. In this paper, we focus on the case of broadband noise. Treating the CM signal as an additional receive signal, we investigate the capacity of the copper cable channel for different levels of coordination among the users. We introduce a channel model which includes the common-mode paths and derive a suitable form of the channel capacity formula. CM crosstalk measurement results, essential for evaluation of the channel capacity, are presented. Using the measurement data, exemplary results of capacity gain achievable by CM-aided data transmission over the copper cable are shown.

## I. INTRODUCTION

Data transmission over copper twisted-pair (TP) cables, standardized as various digital subscriber line (xDSL) technologies, is accomplished by sending and receiving differential-mode (DM) signals. At physical layer level, DM signals appear as a voltage difference  $d(t)$  measured between the two wires, or equivalently, as a current within the loop formed by the TP and the termination impedances, as shown in Fig. 1. The common-mode (CM) signal, in contrast, is the arithmetic mean of the voltages  $c_1(t)$  and  $c_2(t)$ , measured between each wire and ground. The corresponding CM currents appear in the loops formed by each wire, the CM termination impedances, and ground.

Any interference present on the DM receive side of the line, caused by radio signals from wireless services or by neighbouring pairs due to electromagnetic coupling between the wires in the cable, will also cause a corresponding CM component [1]. This is exploited for mitigation of narrowband interference caused by broadcast radio stations or amateur radio transmitters—a kind of interference referred to as radio frequency interference (RFI) ingress in xDSL technologies. The CM signal serves as a reference used for generating a counter

Thomas Magesacher is with the Telecommunications Research Center Vienna (ftw.), Austria. He is also a Ph.D. student at BridgeLab, LIS, Munich University of Technology, Germany.

Dr. Per Ödler is a Docent at Lund Institute of Technology, Department of Electrosience, Sweden.

Dr. Per Ola Börjesson is a Professor of Signal Processing at Lund Institute of Technology, Department of Electrosience, Sweden.

Dr. Werner Henkel and Dr. Tomas Nordström are senior researchers with the Telecommunications Research Center Vienna (ftw.), Austria.

Roland Zukunft and Sven Haar are with BridgeLab, LIS, Munich University of Technology, Germany.

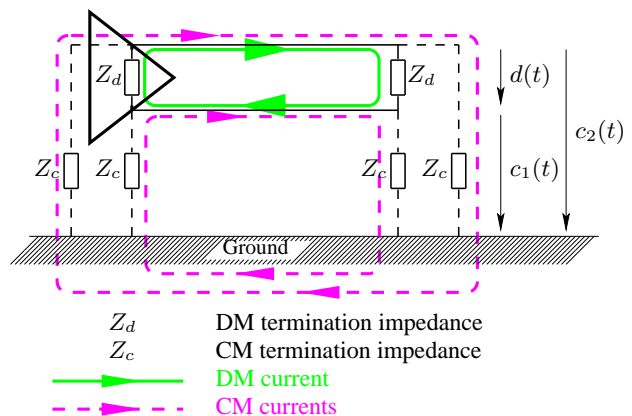


Fig. 1. DM and CM currents and voltages in a wireline transmission system.

interferer, which is then subtracted from the DM receive signal. This CM-reference based approach benefits from the strong and clear appearance of the interferer on the CM. Narrowband-interference suppression levels of up to 30 dB are achievable in practice [2],[3].

In this paper, we investigate the theoretical bound on performance gain achieved by using the CM component at the receiver. In general, the CM loop is more susceptible to electromagnetic ingress than the DM loop, since its area is larger. This potentially higher noise level lowers the chances that the CM signal could be useful for interference mitigation of broadband noise. Almost all installed multi-pair cables, however, are shielded, which substantially reduces the amount of noise that enters the cable. Thus the CM signals mainly comprise crosstalk signals from neighbouring pairs, which may be valuable for interference mitigation schemes.

This work is motivated by the need for fundamental understanding of the potential increase of throughput using CM signals on the receive side. Our goal is to investigate an approach for achieving gain in capacity by CM-aided transmission. To determine the gain, cable measurement results are used.

In Section II we start with the discrete-time representation of a continuous-time channel and introduce a channel model that includes the CM components present in the cable. A suitable expression for the channel capacity is derived in Section III. Supporting cable measurements are described in Section IV. Channel capacity gain results for an example scenario are presented in Section V.

## II. CHANNEL MODEL

We introduce a general time-domain channel model without assuming any particular modulation type or even synchronized transmission of all the users.

### A. Discrete-Time Model of the Continuous-Time Channel

Let  $x_i(t)$  denote the signal transmitted over the  $i$ -th TP of a  $K$ -pair cable. The linear channel is described by its impulse response  $h(t)$  and is assumed to be causal and of finite length  $T_h$ , i.e.,  $h(t) = 0$  for  $t < 0$  and  $t > T_h$ . Furthermore, we consider the channel to be time-invariant during transmission of our signal segment of interest. This is a reasonable assumption for wireline channels, which change their transmission properties due to slowly varying parameters, like, e.g., temperature. The segment of interest of the transmitted signal,  $x_i(t)$  for  $0 \leq t \leq T_x$ , will affect the channel output  $y_i(t)$  for  $0 \leq t \leq T_x + T_h$  as a result of continuous-time convolution:

$$y_i(t) = \int_{\tau=-T_h}^{T_x+T_h} x_i(\tau)h(t-\tau)d\tau, \quad 0 \leq t \leq T_x+T_h. \quad (1)$$

Note that we assume continuous data transmission preceding and succeeding our segment of interest, i.e.,  $x_i(t) \neq 0$  for  $t < 0$  or  $t > T_x$ . Equidistant sampling of (1) with a sampling period  $T$  yields

$$y_i[n] = \sum_{m=-(N-1)}^{L+N-2} x_i[m]h[n-m], \quad 0 \leq n \leq L+N-2, \quad (2)$$

where  $n$  is the discrete-time index,  $N = \lfloor \frac{T_x}{T} \rfloor$  is the channel length in terms of sampling periods,  $L = \lfloor \frac{T_x}{T} \rfloor$  is the length of the transmit segment of interest, and  $\lfloor \cdot \rfloor$  denotes the largest integer smaller than or equal to the argument. The convolution sum for a block of samples in (2) written in matrix form is

$$\underbrace{\mathbf{y}_i}_{(L+N-1) \times 1} = \underbrace{\mathbf{H}}_{(L+N-1) \times (L+2N-2)} \cdot \underbrace{\mathbf{x}_i}_{(L+2N-2) \times 1}. \quad (3)$$

The channel convolution matrix is a Toeplitz matrix

$$\mathbf{H} = \begin{bmatrix} \mathbf{h}^T & 0 & \cdots & 0 \\ 0 & \mathbf{h}^T & \cdots & 0 \\ \vdots & & \ddots & \vdots \\ 0 & \cdots & 0 & \mathbf{h}^T \end{bmatrix}, \quad (4)$$

where the discrete-time channel impulse response of length  $N$  is given by

$$\mathbf{h} = [h[0] \cdots h[N-1]]^T. \quad (5)$$

The input signal vector  $\mathbf{x}_i = [\mathbf{x}_s^T \ \mathbf{x}_a^T \ \mathbf{x}_p^T]^T$  contains  $L+2N-2$  samples that affect  $L+N-1$  samples of the output signal block  $\mathbf{y}_i = [y_i[L+N-2] \cdots y_i[0]]^T$ . The actual transmit segment of interest is  $\mathbf{x}_a = [x_i[L-1] \cdots x_i[0]]^T$ , while its preceding

$N-1$  samples are collected in  $\mathbf{x}_p = [x_i[-1] \cdots x_i[N-1]]^T$ , and its succeeding  $N-1$  samples constitute the vector  $\mathbf{x}_s = [x_i[L-N-2] \cdots x_i[L]]^T$ . Summarizing, a block of  $L$  input samples  $\mathbf{x}_a$  transmitted over a channel of length  $N$  affects  $L+N-1$  output samples, themselves affected by  $N-1$  preceding and  $N-1$  succeeding transmit samples with respect to  $\mathbf{x}_a$ . Aiming at the average capacity, which we would obtain observing blocks of length  $L \rightarrow \infty$ , we choose  $L \gg N$ , with the computational complexity as constraint.

### B. Coordinated Transmission: Vector Channel Model

In case an operator has the possibility to use all the TPs in a cable and all line ends are colocated on either one or both sides, data transmission over the individual TPs can be done in a coordinated way. The copper cable is then viewed as a multiple-input multiple-output (MIMO) channel. A MIMO scheme for colocated transceivers on both sides is proposed in [4], an approach for the one-sided case is presented in [5].

The  $K$  DM output vectors  $\mathbf{d}_i$  and the  $K$  CM output vectors  $\mathbf{c}_i$  of the TPs are stacked to form the output vector  $\mathbf{y}$  of the channel as shown in (6). The  $K$  input vectors  $\mathbf{x}_i$  are collected in the vector  $\mathbf{x}$ . The input-output relation of the linear channel is modelled by the convolution matrices  $\mathbf{H}_{i,j}^{(d)}$  and  $\mathbf{H}_{i,j}^{(c)}$ , which describe the transfer paths from DM input  $j$  to DM output  $i$  and CM output  $i$ , respectively. For a compact representation these matrices are collected in the matrix  $\mathbf{H}_x$ .

The noise introduced by the channel is modelled by  $M+2K$  independent noise sources, where  $M$  is the number of sources represented by the vectors  $\mathbf{v}_i$ , which cause mutually dependent noise components at the DM and CM outputs of each TP. The influence of noise source  $j$  on the DM and CM receive signals of TP  $i$  is described by the convolution matrices  $\mathbf{H}_{i,j}^{(vd)}$  and  $\mathbf{H}_{i,j}^{(vc)}$ , respectively. For example,  $K$  out of the  $M$  sources model NEXT. External noise sources, with regard to the shielded cable, like radio disturbers, also cause mutually dependent noise components at the output of the individual TPs.

Apart from the  $M$  dependent noise components there are also  $2K$  independent noise components, one at the DM and one at the CM output of each TP. Independent noise is made up of background noise and noise generated by the distinct analog front-ends at each TP. We model the independent noise by  $K$  noise vectors  $\mathbf{v}_i^{(d)}$  for the DM and  $K$  noise vectors  $\mathbf{v}_i^{(c)}$  for the CM. Their corresponding convolution matrices are  $\mathbf{H}_i^{(vd)}$  and  $\mathbf{H}_i^{(vc)}$ , respectively. All the noise convolution matrices form  $\mathbf{H}_v$ . The correspondence between the elements of our model and the physical paths in the cable is summarized in Table I. Convolution matrices  $\mathbf{H}_{i,j}^{(vd)}$ ,  $\mathbf{H}_{i,j}^{(vc)}$  with  $j > K$  model the paths from external interferers, like, e.g., radio transmitters.

### C. Uncoordinated Transmission: Single-Pair Model

In case of no coordination among the users, the output of the  $k$ -th TP can be derived from the vector channel model (6)

$$\underbrace{\begin{bmatrix} d_1 \\ \vdots \\ d_K \\ c_1 \\ \vdots \\ c_K \end{bmatrix}}_{\mathbf{y}} = \underbrace{\begin{bmatrix} \mathbf{H}_{1,1}^{(d)} \cdots \mathbf{H}_{1,K}^{(d)} \\ \vdots \ddots \vdots \\ \mathbf{H}_{K,1}^{(d)} \cdots \mathbf{H}_{K,K}^{(d)} \\ \mathbf{H}_{1,1}^{(c)} \cdots \mathbf{H}_{1,K}^{(c)} \\ \vdots \ddots \vdots \\ \mathbf{H}_{K,1}^{(c)} \cdots \mathbf{H}_{K,K}^{(c)} \end{bmatrix}}_{\mathbf{H}_x} \underbrace{\begin{bmatrix} \mathbf{x}_1 \\ \vdots \\ \mathbf{x}_K \end{bmatrix}}_{\mathbf{x}} + \underbrace{\begin{bmatrix} \mathbf{H}_{1,1}^{(vd)} \cdots \mathbf{H}_{1,M}^{(vd)} & \mathbf{H}_1^{(vd)} \cdots \mathbf{0} & \mathbf{0} \cdots \mathbf{0} \\ \vdots \ddots \vdots & \vdots \ddots \vdots & \vdots \ddots \vdots \\ \mathbf{H}_{K,1}^{(vd)} \cdots \mathbf{H}_{K,M}^{(vd)} & \mathbf{0} \cdots \mathbf{H}_K^{(vd)} & \mathbf{0} \cdots \mathbf{0} \\ \mathbf{H}_{1,1}^{(vc)} \cdots \mathbf{H}_{1,M}^{(vc)} & \mathbf{0} \cdots \mathbf{0} & \mathbf{H}_1^{(vc)} \cdots \mathbf{0} \\ \vdots \ddots \vdots & \vdots \ddots \vdots & \vdots \ddots \vdots \\ \mathbf{H}_{K,1}^{(vc)} \cdots \mathbf{H}_{K,M}^{(vc)} & \mathbf{0} \cdots \mathbf{0} & \mathbf{0} \cdots \mathbf{H}_K^{(vc)} \end{bmatrix}}_{\mathbf{H}_v} \underbrace{\begin{bmatrix} \mathbf{v}_1 \\ \vdots \\ \mathbf{v}_M \\ \mathbf{v}_1^{(d)} \\ \vdots \\ \mathbf{v}_K^{(d)} \\ \mathbf{v}_1^{(c)} \\ \vdots \\ \mathbf{v}_K^{(c)} \end{bmatrix}}_{\mathbf{v}} \quad (6)$$

$$\underbrace{\begin{bmatrix} d_k \\ c_k \end{bmatrix}}_{\mathbf{y}} = \underbrace{\begin{bmatrix} \mathbf{H}_{k,k}^{(d)} \\ \mathbf{H}_{k,k}^{(c)} \end{bmatrix}}_{\mathbf{H}_x} \underbrace{\begin{bmatrix} \mathbf{x}_k \end{bmatrix}}_{\mathbf{x}} + \underbrace{\begin{bmatrix} \mathbf{H}_{k,1}^{(d)} \cdots \mathbf{H}_{k,(k-1)}^{(d)} & \mathbf{H}_{k,(k+1)}^{(d)} \cdots \mathbf{H}_{k,K}^{(d)} \cdots \mathbf{H}_{k,M}^{(vd)} & \mathbf{H}_k^{(vd)} & \mathbf{0} \\ \mathbf{H}_{k,1}^{(c)} \cdots \mathbf{H}_{k,(k-1)}^{(c)} & \mathbf{H}_{k,(k+1)}^{(c)} \cdots \mathbf{H}_{k,K}^{(c)} \cdots \mathbf{H}_{k,M}^{(vc)} & \mathbf{0} & \mathbf{H}_k^{(vc)} \end{bmatrix}}_{\mathbf{H}_v} \underbrace{\begin{bmatrix} \mathbf{x}_1 \\ \vdots \\ \mathbf{x}_{k-1} \\ \mathbf{x}_{k+1} \\ \vdots \\ \mathbf{x}_K \\ \vdots \\ \mathbf{v}_M \\ \mathbf{v}_k^{(d)} \\ \mathbf{v}_k^{(c)} \end{bmatrix}}_{\mathbf{v}} \quad (7)$$

by extracting the corresponding two rows as formulated in (7). The transmit signals of neighbouring pairs, if present, represent  $K - 1$  of the  $M$  noise sources that cause mutually dependent components on DM and CM.

### III. CHANNEL CAPACITY

Starting from the generic channel model  $\mathbf{y} = \mathbf{H}_x \mathbf{x} + \mathbf{H}_v \mathbf{v}$ , that has been refined for two special cases in (6) and (7), the channel capacity is defined as the maximum mutual information

of the two random vectors  $\mathbf{y}$  and  $\mathbf{x}$  [6]:

$$C = \max_{\text{pdf}(\mathbf{x}), \sigma_x^2 = \text{const.}} \{\mathbb{I}(\mathbf{y}, \mathbf{x})\}. \quad (8)$$

Maximization is performed over all probability density functions of  $\mathbf{x}$  with a given finite variance  $\sigma_x^2$ . Assuming that the channel is known in the receiver, the covariance matrix of the zero-mean Gaussian distributed transmit vector  $\mathbf{x}$  is

$$\mathbf{C}_{xx} = \mathbb{E}\{\mathbf{x}\mathbf{x}^T\} = \sigma_x^2 \mathbf{I}. \quad (9)$$

We further assume that all elements of the noise vector  $\mathbf{v}$  are uncorrelated and Gaussian distributed with zero mean. The covariance matrix of the channel output vector is

$$\mathbf{C}_{yy} = \mathbb{E}\{\mathbf{y}\mathbf{y}^T\} = \mathbf{H}_x \mathbf{C}_{xx} \mathbf{H}_x^T + \mathbf{H}_v \mathbf{C}_{vv} \mathbf{H}_v^T. \quad (10)$$

The covariance matrix of the noise in, e.g., (6), is given by

$$\mathbf{C}_{vv} = \text{diag}\left\{\left[\sigma_1^2 \cdots \sigma_M^2 \sigma_1^{(d)2} \cdots \sigma_K^{(d)2} \sigma_1^{(c)2} \cdots \sigma_K^{(c)2}\right]\right\} \otimes \mathbf{I}_{L+2N-2}, \quad (11)$$

where  $\text{diag}\{\cdot\}$  denotes the diagonal matrix with the argument vector on the main diagonal,  $\otimes$  is the Kronecker product, and  $\mathbf{I}_k$  is the  $k \times k$  identity matrix. Since the channel is linear,  $\mathbf{x}$  and  $\mathbf{y}$  are jointly Gaussian distributed and we write their mutual information as in [7]:

$$\mathbb{I}(\mathbf{y}, \mathbf{x}) = \frac{1}{2} \log \left( \frac{\det(\mathbf{C}_{xx}) \det(\mathbf{C}_{yy})}{\det(\mathbf{C}_{zz})} \right), \quad z = \begin{bmatrix} \mathbf{y} \\ \mathbf{x} \end{bmatrix}. \quad (12)$$

| model                     | path represented in the cable ( $i, j = 1, \dots, K$ ) |
|---------------------------|--|
| $\mathbf{H}_{i,i}^{(d)}$  | DM to DM path of TP $i$                                |
| $\mathbf{H}_{i,j}^{(d)}$  | FEXT path from TP $j$ to TP $i$                        |
| $\mathbf{H}_{i,i}^{(vd)}$ | Echo path of TP $i$                                    |
| $\mathbf{H}_{i,j}^{(vd)}$ | NEXT path from TP $j$ to TP $i$                        |
| $\mathbf{H}_{i,i}^{(c)}$  | DM to CM path of TP $i$                                |
| $\mathbf{H}_{i,j}^{(c)}$  | DM to CM FEXT path from TP $j$ to TP $i$               |
| $\mathbf{H}_{i,i}^{(vc)}$ | CM echo path of TP $i$                                 |
| $\mathbf{H}_{i,j}^{(vc)}$ | CM NEXT path from TP $j$ to TP $i$                     |

TABLE I

CORRESPONDENCE BETWEEN THE ELEMENTS OF OUR MODEL AND THE PHYSICAL PATHS IN THE CABLE.

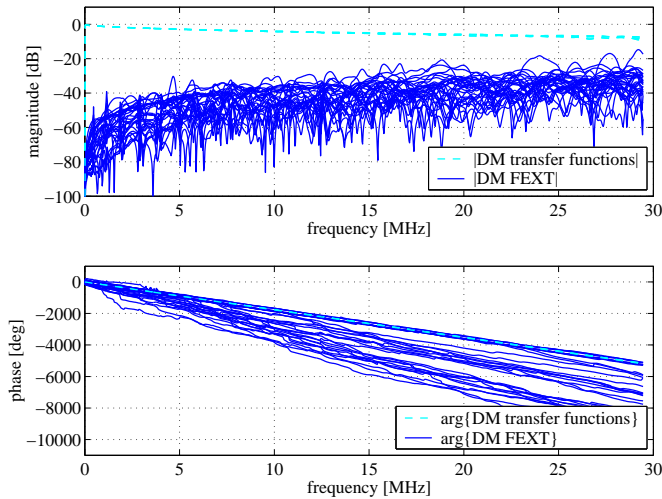


Fig. 2. Measured DM transfer functions (6 in total) and DM FEXT transfer functions (30 in total), which yield the convolution matrices  $\mathbf{H}_{i,j}^{(d)}$  for a 6-pair cable.

We denote the covariance matrix of the auxiliary vector  $\mathbf{z}$  by  $\mathbf{C}_{zz}$ . The mutual information is given by

$$I(\mathbf{y}, \mathbf{x}) = \frac{1}{2} \log \left( \frac{\det(\mathbf{H}_x \mathbf{C}_{xx} \mathbf{H}_x^T + \mathbf{H}_v \mathbf{C}_{vv} \mathbf{H}_v^T)}{\det(\mathbf{H}_v \mathbf{C}_{vv} \mathbf{H}_v^T)} \right). \quad (13)$$

Since Gaussian distribution of the input signal maximizes (8), the channel capacity  $C$  corresponds to the mutual information.

#### IV. CABLE MEASUREMENTS

For evaluation of the channel capacity using the analytical result (13) it is essential to apply real data for the convolution matrices. Since there are no established crosstalk models for the CM path, as it is the case for the DM path [8], we measure the frequency-domain transfer functions (both magnitude and phase) with a resolution of 8192 points in the range from 0 MHz to 30 MHz, as described in [9]. The impulse responses and convolution matrices are obtained from the transfer functions using the inverse discrete Fourier transform (IDFT).

As an example we chose a 0.6 mm cable with 6 pairs (vendor identification: F02YHJ2Y, PMD6x2x0.6) of length 100 m. The TPs' DM transfer functions are shown together with the DM FEXT transfer functions in Fig. 2. CM transfer functions and CM FEXT transfer functions are shown in Fig. 3.

CM FEXT is at least as strong as DM FEXT and is, depending on the frequency range, up to 10 dB stronger. Conversion from DM at one side to CM at the other side of the cable, described by the CM transfer functions, yields CM components in the same order of magnitude as the CM FEXT.

#### V. EXEMPLARY CHANNEL CAPACITY RESULTS

We demonstrate the evaluation of (13) for two example scenarios of uncoordinated transmission over the 6-pair cable. Since we assume a frequency division duplexing scheme, which

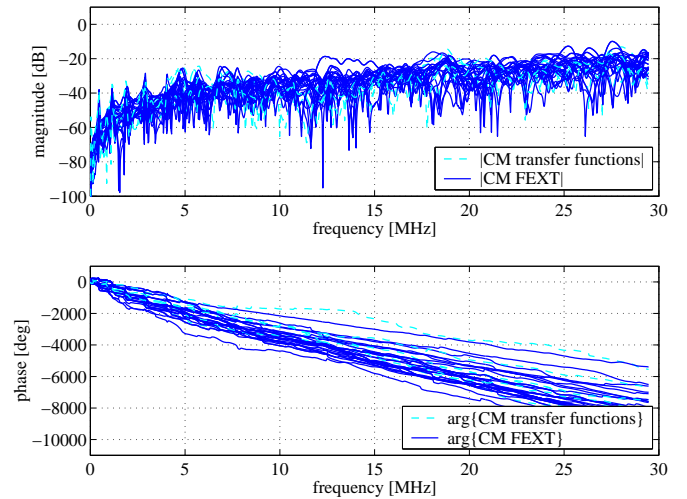


Fig. 3. Measured CM transfer functions (6 in total) and CM FEXT transfer functions (30 in total), which yield the convolution matrices  $\mathbf{H}_{i,j}^{(c)}$  for a 6-pair cable.

is employed, *e.g.*, in VDSL, NEXT is negligible. CM and DM background noise, as well as the transmit signal, are assumed white. We denote the ratio of DM background noise power level and signal power level by  $\alpha$ , *i.e.*,  $\alpha$  is inversely proportional to the signal-to-noise ratio (SNR) at the receiver input. The ratio of CM background noise power level and signal power level is denoted by  $\beta$ .

In order to assess the scenarios we define the relative capacity gain  $\Delta \text{Capacity} = \frac{C_{\text{DM-CM}} - C_{\text{DM}}}{C_{\text{DM}}}$ , where  $C_{\text{DM-CM}}$  and  $C_{\text{DM}}$  is the capacity achieved by joint CM-DM processing and conventional DM processing, respectively.

##### A. Scenario 1: FEXT Disturber

As a first scenario we consider a single strong FEXT disturber, which represents the closest transmitting modem on the opposite side of the cable. As shown in Fig. 4, the capacity gain increases towards high DM noise power levels ( $\alpha > 10^{-2}$ ) in case the CM noise power levels are small. This indicates that transmission is rather done via the CM than the DM in that case. These noise levels, however, constitute a scenario of low practical relevance. With increasing SNR levels ( $\alpha < 10^{-2}$ ) the capacity gain rises since the disturber is (at least partly) cancelled if both CM and DM signals are available. The dotted lines show the capacity gain for constant DM and CM background noise power level ratios ( $\alpha/\beta = \text{const}$ ), *i.e.*,  $\alpha/\beta = 1$  denotes the scenario when CM and DM background noise are equally strong. Receiver operating points encountered in practice typically lie below this curve. A capacity gain of up to 45% is achieved for high SNR and low CM background noise power levels.

##### B. Scenario 2: Wireless Interference

The second scenario is motivated by the radio frequency interference (RFI) problem in DSL: amateur radio transmitters

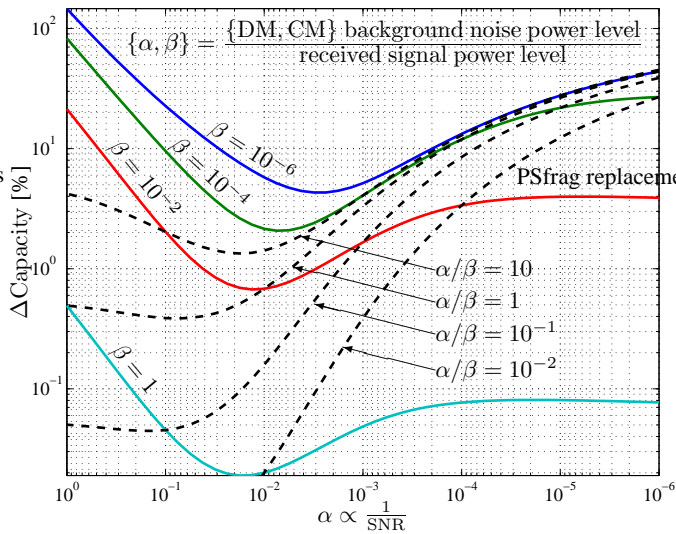


Fig. 4. Channel capacity gain in scenario 1 (one FEXT disturber with equal transmit power compared to the transmit signal).

and broadcast radio stations may cause strong interference levels at the receiver input. Although these wireless sources are of rather narrow bandwidth, we consider a stationary wireless interference source of 3 MHz bandwidth centered at 7.5 MHz, in order to create severe interference. Different coupling from the source to the receiver's DM and CM input is assumed. The relative power spectral densities of DM and CM are depicted in Fig. 5. The CM interference is typically stronger than its DM counterpart, which has two reasons: firstly, the CM loop, formed by the two wires and ground, is larger than the DM loop, and secondly, the wires are usually twisted. We assume the CM ingress 20 dB stronger than the DM ingress, whose power equals the receive signal power.

The capacity gain, as shown in Fig. 6, amounts up to 50% and follows the same trend as in the previous case, apart from the declining capacity gain of the  $\beta = 1$  curve for increasing SNR. This simply indicates that, in the presence of very strong CM noise, the capacity increase with rising SNR is higher in case of pure DM processing compared to joint CM-DM processing.

## VI. SUMMARY AND CONCLUSION

The focus of this paper is on the CM signals and their impact on the throughput in wireline data transmission. We introduce

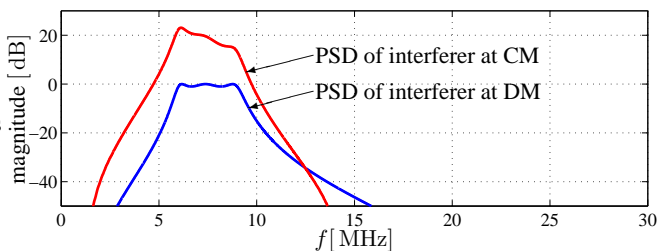


Fig. 5. Scenario 2: relative power spectral density (PSD) of the band limited wireless interferer at the receiver input.

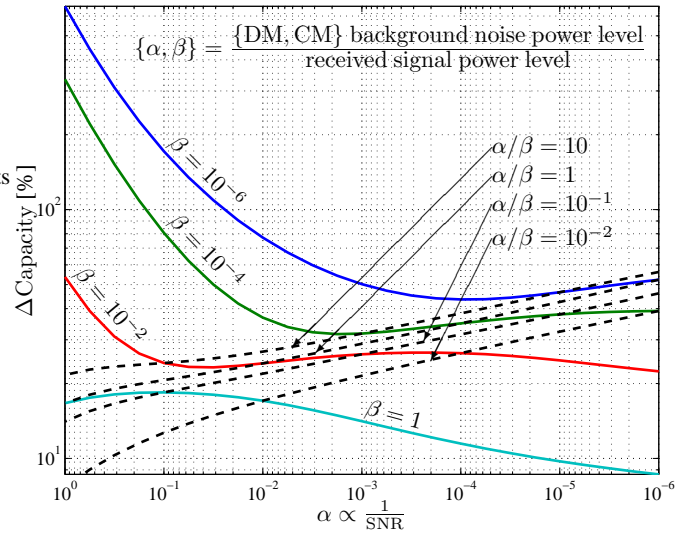


Fig. 6. Channel capacity gain in scenario 2 (single band limited wireless disturber, which appears 20 dB stronger on CM input compared to DM input). Note, that the scaling of the y-axis is different than in Fig. 4.

a channel model that includes the CM and derive a suitable expression for the channel capacity formula. Results of CM crosstalk measurements, the basis for capacity considerations, are presented. Based on these results we evaluate the channel capacity gain using the CM signals on the receive side. We show that scenarios with high SNR levels and low CM noise power levels benefit significantly from exploiting the CM signal at the receiver.

## ACKNOWLEDGMENT

We are very grateful to Petr Kadlec for his support during the measurement campaign and we thank Maja Lončar for her valuable comments during numerous discussions.

## REFERENCES

- [1] T. Magesacher, W. Henkel, T. Nordström, P. Ödling, and P. O. Börjesson, "On the Correlation between Common-Mode and Differential-Mode Signals," *Temporary Document TD 45, 013145, ETSI STC TM6*, Sept. 2001.
- [2] T. Magesacher, P. Ödling, T. Nordström, T. Lundberg, M. Isaksson, and P. O. Börjesson, "An Adaptive Mixed-Signal Narrowband Interference Canceller for Wireline Transmission Systems," in *Proc. IEEE Int. Symp. Circuits and Systems*, Sydney, Australia, May 2001, vol. IV, pp. 450–453.
- [3] P. Ödling, P. O. Börjesson, T. Magesacher, and T. Nordström, "An Approach to Analog Mitigation of RFI," *IEEE J. Select. Areas Commun.*, vol. 20, no. 5, pp. 974–986, June 2002.
- [4] G. Tauböck and W. Henkel, "MIMO Systems in the Subscriber-Line Network," in *Proc. Fifth Int. OFDM Workshop*, Hamburg, Germany, Sept. 2000, pp. 18.1–18.3.
- [5] G. Ginis and J. M. Cioffi, "Vectored Transmission for Digital Subscriber Line Systems," *IEEE J. Select. Areas Commun.*, vol. 20, no. 5, pp. 1085–1104, June 2002.
- [6] T. M. Cover and J. A. Thomas, *Elements of Information Theory*, John Wiley and Sons, ISBN 0-471-06259-6, 1991.
- [7] M. S. Pinsky, *Information and Information Stability of Random Processes*, Holden Day, 1964.
- [8] C. Valenti, "NEXT and FEXT Models for Twisted-Pair North American Loop Plant," *IEEE J. Select. Areas Commun.*, vol. 20, no. 5, pp. 893–900, June 2002.
- [9] T. Magesacher, W. Henkel, G. Tauböck, and T. Nordström, "Cable Measurements Supporting xDSL Technologies," *Journal e&i Elektrotechnik und Informationstechnik*, vol. 199, no. 2, pp. 37–43, Feb. 2002.